SHAKING TABLE TESTS OF DYNAMIC INTERACTION OF SOIL-STRUCTURE CONSIDERING SOIL LIQUEFACTION

Peizhen Li[1], Hongmei Ren[2], Xilin Lu[3] and Lei Cheng[2]

[1] *Associate Professor, State Key Lab. for Disaster Reduction in Civil Eng., Tongji Univ., Shanghai, China*
[2] *PH.D student, State Key Lab. for Disaster Reduction in Civil Eng., Tongji Univ., Shanghai, China*
[3] *Professor, State Key Lab. for Disaster Reduction in Civil Eng., Tongji Univ., Shanghai, China*
Email: lipeizh@mail.tongji.edu.cn

ABSTRACT:

Shaking table model tests on soil-structure interaction system in liquefiable ground are described in this paper. A flexible container was fabricated to minimize the box effect. Pile foundation was used in the test. A 12-story cast-in-place R.C. frame model was used as superstructure, and sand soil was employed as model soil. In the tests, macro-phenomena of soil liquefaction and structure failure due to natural earthquake were reproduced well. The natural frequency of interaction system decreased and the damping ratio of soil increased with the increase of the shaking. The liquefied soil could filter and isolated vibration. The phenomena of transient minus pore pressure occurred in the test. Pore water pressure did not always dissipate in short time immediately after the excitations, but it may keep on increasing too. The distribution of the strain amplitude along the pile was the shape where the large strain was at the top of the pile and the small strain was at the tip of the pile. And the distribution of the contact pressure on the pile-soil interface was related to the excitation magnitude.

KEYWORDS: sand soil, liquefaction, interaction, shaking table test, seismic response

1. INTRODUCTION

Dynamic test on soil-structure interaction (SSI) in liquefied grounds is one of the highlights of SSI studies, but is also recognized to be very challenging. Researchers have derived a lot of valuable conclusions from shaking table scale model tests of SSI in liquefied ground (e.g., Funahara et al. 2000, Kagawa et al. 2000, Tamura et al .2000, Takahiro et al. 2004, Chen et al. 2003, Feng et al. 2005, Meng et al. 2005, Ling et al. 2006). With the development of model similitude theory and structural seismic testing technology, shaking table model test has played more and more important role on the research of SSI. However, this kind of test is rather difficult due to its complexity. To our knowledge, these tests have not yet been attempted on tall structural systems (12 floors and above) supported by piles embedded in liquefiable soils.

The test on soil-pile-structure interaction system considering the soil liquefaction was carried out in State Key Laboratory for Disaster Reduction in Civil Engineering, Tongji University, China, in June 2007. The dynamic responses of soils and structures during earthquake shakings were documented by accelerometers, displacement meter and strain gauges, attached to the structures and embedded in the soils surrounding the structures. And pore pressure gauges were embedded in soil to measure the change of pore pressure. This paper gives the results from the shaking table tests.

2. BRIEF DESCRIPTION OF SHAKING TABLE MODEL TESTS

2.1 Similitude Design of Models

To study the seismic characteristics and response of the dynamic SSI system, the similitude design of test models is based on the following principles (Sabnis et al.1983, Lu et al. 1999). (1) The same similitude relation was applied to soil, foundation and superstructure. (2) Distortion of gravity was permitted. The method of adding additional weight was not adopted in present study in that it was almost impossible to be realized in soil and pile foundations. (3) Parameters of dynamic loads were controlled to meet the performance requirements of shaking table. (4) Requirements of construction and capacity of equipment must be accessible in laboratory.

Consequently, non-gravity model with similitude rules controlled materials was adopted in present test. Similitude formulas and similitude factors of all physical quantities were induced from Bockingham π theorem. A 12-story cast-in-place frame was used as prototype superstructure, and sand soil was selected as prototype soil. The scales of models were 1/10. The similitude factor of mass density was 1, and the similitude factor of elasticity modulus for structure was 1/2.668.

2.2 Similitude Design of Models

In the shaking table model test, the model soil should be held in a box of reasonable size. Because of wave reflection on the boundary, an error called boundary effects will affect the test results. To reduce the boundary effect, a flexible container and proper constructional details were designed for the model test, and the ratio of the ground plane diameter to the structural plane diameter (i.e., D/d) was set at 5 by controlling the size of the structural plane. The cylindrical container was 3000 mm in diameter, and its lateral rubber membrane was 5 mm thick. Reinforcement loops of 4 mm diameter, spaced at 60 mm, were used to strengthen the outside of the container in the tangential direction (Lu et al. 2005).

2.3 Design and Fabrication of the Models

Saturated sand covered by silt clay was used for the soil model. The top layer was silt clay, 0.2m in depth; while the bottom layer was sand, 1.30m in depth. For the foundation of the superstructure, nine piles of a pile group were used. The pile was 0.9m in length. The superstructure had a 12-story reinforced concrete frame, with a single bay and a single span. Foundation and soil were designed according to the similitude relation. The scaling factors was 1/10. The superstructure and foundation was made of micro-concrete and fine zinc-coated steel bar. Properties of all materials were measured by material tests before the shaking table test.

2.4 Arrangement of Measuring Points

Accelerometers, displacement meter and strain gauges were used to measure the dynamic response of the superstructure, foundation and soil. Pore pressure gauges were embedded in soil to measure the change of pore pressure. Pressure gauges were used to measure the contact pressure between piles and the surrounding soil. Fig.1 shows the arrangement of measuring points.

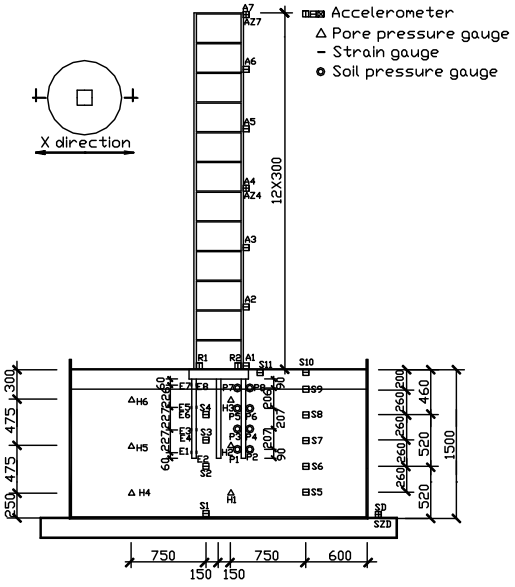

Fig.1 Sketch of the measuring point arrangement of test

2.5 Test Loading Schedules

Ground shaking was simulated as unidirectional (x direction of the shaking table). The records selected for the study included (i) a record from the 1940 El Centro earthquake; (ii) a synthetically generated record (Shanghai Bedrock wave). Fig.2~Fig.3 depict the acceleration time-history and corresponding Fourier spectra of the waves. Five levels of excitation were used in this study. From level 1 to level 5 the values for peak accelerations were, 0.131, 0.375, 0.75, 1.125 and 1.5g, respectively. Before and after the altering of each acceleration level, the White Noise with small amplitude was inputted to observe the change of dynamic characteristics of the system. The time interval for the 1/10 scale test was 0.003266 s. Table 1 gives the test loading program.

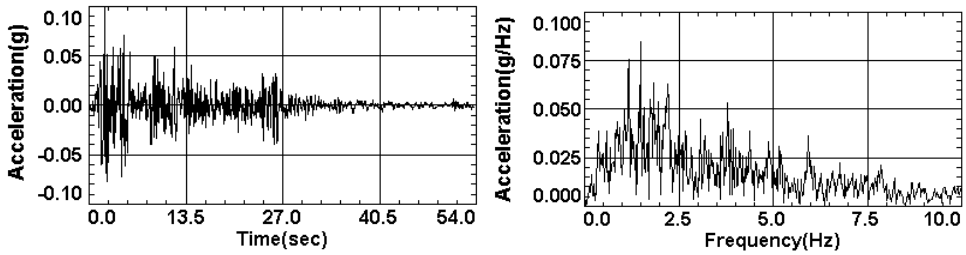

Fig.2 The acceleration time-history and corresponding Fourier spectra of El Centro wave

3. THE RESULTS AND RULES OF THE SHAKING TABLE TEST

3.1 Experimental Phenomena

Fig.4 and Fig.5 show the model used in present test, and we could see there was no water on the surface of soil at this moment. The phenomena water emitting and sand boiling occurred near the container edge and

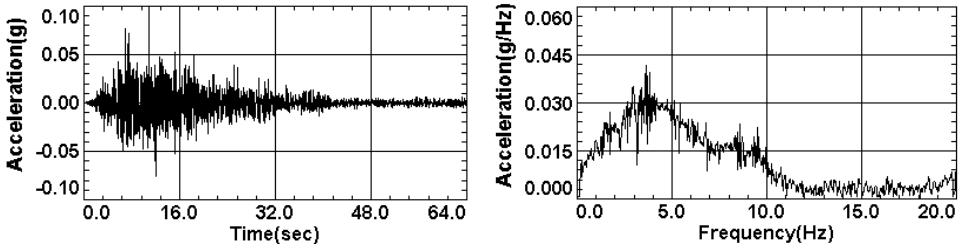

Fig.3 The acceleration time-history and corresponding Fourier spectra of Shanghai Bedrock

Table 1 Test Loading Schedules of test

No.	Excitation code	Acceleration peak value (g)		Remarks
		Prototype	model	
1	1WN	—	0.07	
2、3	EL1、SJ1	0.035	0.131	Basic seismic of 7 degree
4	4WN	—	0.07	
5、6	EL2、SJ2	0.1	0.375	7 degree
7	7WN	—	0.07	
8、9	EL3、SJ3	0.2	0.75	8 degree
10	10WN	—	0.07	
11、12	EL4、SJ4	0.3	1.125	
13	13WN	—	0.07	
14、15	EL5、SJ5	0.4	1.5	
16	16WN	—	0.07	

Note：EL——El Centro wave（unidirectional X）；SJ——Shanghai bedrock wave（unidirectional X）

around the foundation after the excitation of EL2 and lasted about 4.5 minutes. The accumulated water increased slowly where the phenomenon of water emitting occurred and linked into a small area in the east near the container edge and around the foundation after the excitation of SJ2. Sand boiling increased obviously. The water near the eastern edge of the container linked into a large area with the water around the foundation and the southern edge of thee container after the excitation of EL3 (Fig.7). The sand boiled and the accumulated water increased. The superstructure sank a little and inclined northwestwardly slightly. The boiling phenomenon appeared at the northeast corner and the southeast corner of the foundation after the excitation of EL4 and lasted about 3.5minutes. The superstructure inclined southwestwardly at about 8°. The superstructure inclined southwestwardly seriously at about 15° after the excitation of SJ4. The bubbling phenomenon appeared at some sites around the base of the structure. Two sides of the foundation base were below the water and the ground surface was covered wholly by the water. The ground surface and the structure sank obviously. The foundation continued to sink after the excitation of EL5. Four sides and three corners were below the water already. The structure inclined southwestwardly at about 25°. For the great incline of the superstructure, the excitation of SJ6 was not carried out. The superstructure inclined westwardly 20cm and southwardly 30cm after all excitation (See Fig.6). The settlement of the superstructure cap was 11cm at the northeast corner, 13cm at the southeast corner, 12cm at the northwest corner and 19cm at the southwest corner. The depth of the water was 1cm at the northeast corner, 2cm at the southeast corner, 2cm at the northwest corner, 2cm at the southwest corner and 9cm in the container center. The settlement of the ground surface was 3cm at the northeast corner of the container, 2.5cm at the southeast corner, 2cm at the northwest corner, 2cm at the southwest corner and 11cm in the center. Fig.8 shows the settlement and the crack of the surface of the soil after pump out the accumulated water. There was no crack in the superstructure.

The pile was dug out after the test and it could be seen that there were many horizontal cracks along the piles. The crack was dense at the top of the pile and less or none at the tip. The cracks on the two side piles of three rows piles in the vibration direction were much more and larger. However, the cracks on the middle pile were relatively fewer and smaller. The cracks penetrated basically on the plane vertical to the vibration direction and usually did not penetrate on the plane horizontal to the vibration direction. The cracks appeared to be typical bending cracks.

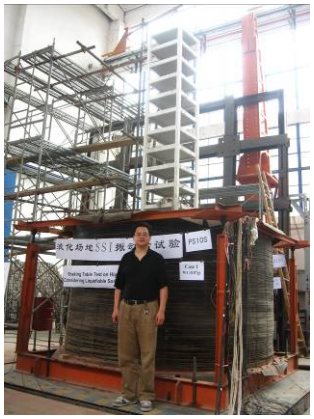

Fig.4 Photo of test

Fig.5 The surface of the soil before test

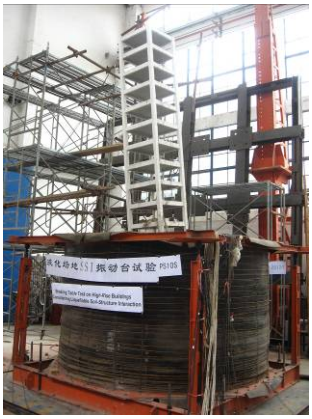

Fig.6 Incline of the structure after test

Fig.7 Water accumulating phenomenon after the excitation of EL3
Fig.8 Accumulated sand and crack in the soil surface after the test

3.2 Dynamic Behavior of Model

Table 2 shows the frequency and damping ratio of the soil and the system under all the excitation according to spectral analysis of the test data. It could be found that the damping ratio of the system was larger than that of the structural material. With the increasing of the vibration times and the excitation peak value, the frequency of the soil and the system decreased while the damping ratio increased. It was results of the soil softening, the rigidity degeneration of the superstructure and the crack development of the pile.

Table 2 The frequency and damping ratio of the soil and the system

No.	Excitation code	Points on the soil surface		Points on the top of superstructure		Freq. of structure on Fixed Base (Hz)
		Freq. (Hz)	Damping ratio (%)	Freq. (Hz)	Damping ratio (%)	
1	1WN	7.443	12.97	2.680	10.16	2.977
4	4WN	7.146	10.67	2.680	11.01	2.977
7	7WN	7.443	13.64	2.382	10.14	2.680
10	10WN	7.443	12.75	2.380	9.26	2.084
13	13WN	6.550	18.74	2.382	8.45	1.489
16	16WN	7.443	13.27	2.382	8.93	1.191

Fig.9 shows the mode shape curve of the model in each phase. It could be seen there exist translational and rotational movement in the foundation because of the soil-structure dynamic interaction. And the main part of the first mode of the superstructure was shear type. The translational movement of the foundation increased with the increasing of the peak acceleration, the pore water pressure of the soil increased and the soil softened. The change of the mode shape curve was small because there was almost no crack appears on the superstructure.

3.3 The Amplification Factors of the Peak Acceleration

Fig.10 shows the curves of relation between the amplification factor and the height of the measuring points in the soil-pile-tall building interaction system in ground of soil liquefaction under different excitation (The amplification factor was the ratio between the peak acceleration of the measuring points and that of measuring

point SD at the container base). The rules could be drawn as follows.

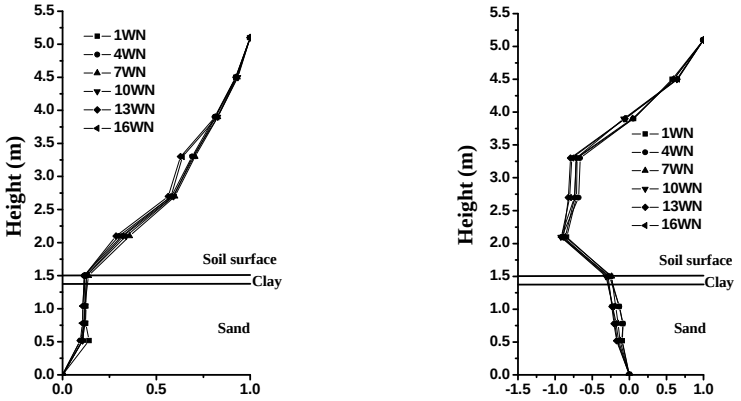

(a) The first mode shape (b) The second mode shape

Fig. 9 Mode shape curves of the model

(1) Magnification or reduction of vibration transferred by soil was related to soil characteristic, excitation magnitude, spectral characteristics of excitation, and so on. Sand magnified vibration under small earthquakes. However, sand soil liquefied, non-linear behavior developed and stiffness declined because of the increasing of the pore water pressure under medium earthquake and strong earthquake. At the time it damped vibration. (2) For the superstructure，the floor peak acceleration was obviously different from each other under small earthquakes. It was the combined result of the multi-mode response of the structure and the structure response caused by the translation and rotation of the foundation. The structure response was small because the soil isolated the vibration obviously under strong earthquake. (3) The amplification factors of the peak acceleration decreased with the peak acceleration of inputted excitation increased. The reason was that the pore water pressure increased, the soil soften continuously, the non-linear of soil developed，the ability to transfer the vibration weakened with the increasing of the excitation times and the intensifying of the inputted excitation.

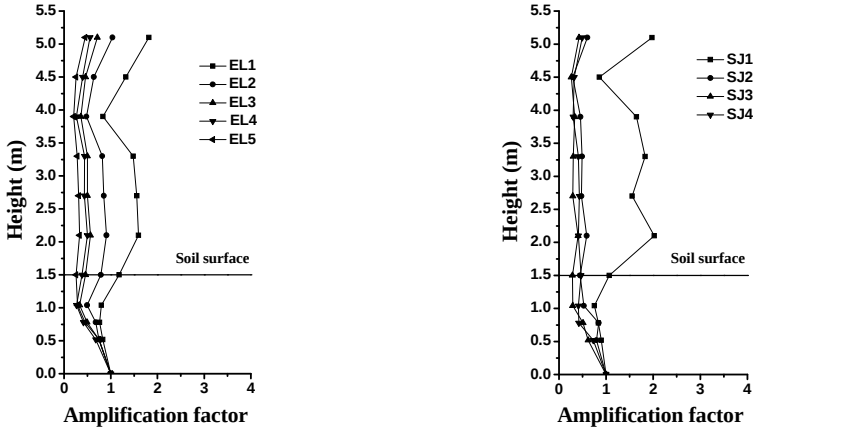

(a) Under excitation of El Centro wave (b) Under excitation of Shanghai Bedrock wave

Fig.10 The amplification factors of the peak acceleration at different heights

3.4 The Transient Variation of the Pore Pressure Ratio in the Soil

The change of pore water pressure in the sand soil was obtained by nine high-sensitivity pore water pressure gauge embedded in the sand soil (The arrangement of the measuring points is shown in Fig.1). In this section, some data of the pore water pressure were given and changing rules of the pore water pressure were studied. And then the change mechanism of the soil behavior in dynamic SSI system was studied.

Fig.11 shows the pore pressure ratio time history at different measuring points under the excitation of SJ4. (The arrangement of the time history figure was consistent with relative position of the measuring points and the figure was after correction of zero lin. The initial 3.344s was the time to heat up the shaking table.) From the figure, we could draw the rules as follows.

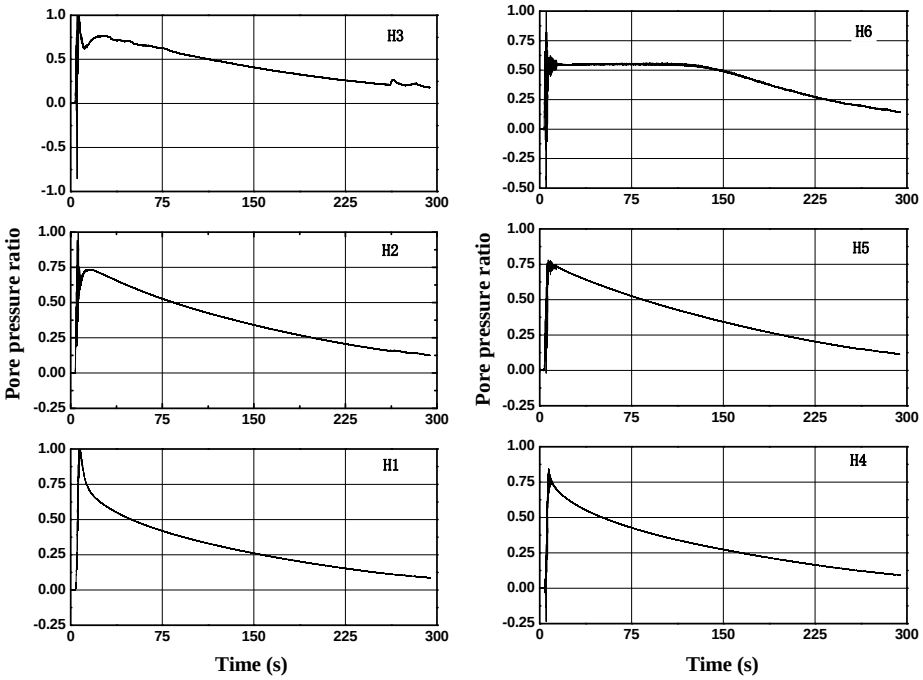

Fig.11 The pore pressure ratio time history of different measuring points under excitation of SJ4

(1) From the figure it could be seen that the pore water pressure in the sand layer builds up gradually with the large cycles of acceleration in the case of small and large earthquakes. The pore pressure ratio mainly dissipated after the excitation and the velocity of the dissipation tended to slow gradually from top to bottom. (2) The pore water pressure and the pore pressure ratio increased with the increasing the peak acceleration of the imputed excitation except the measuring points which the pore pressure ratio reach to 1. (3) It could also be seen that the transient negative pore pressure occurred when the initial acceleration reached the peak value. The main reason was that the sand soil layer performed transient swelling effect when the initial acceleration reached the peak value. So it was not pressure but suction at the moment and the transient value obtained by the pore water pressure gauge was negative. (4) The value of the pore water pressure and the pore pressure ratio had relation with the depth and the location whether the measuring point lay below the foundation. For the measuring points at the same depth, the value of the pore water pressure and the pore pressure ratio lying below the foundation was obviously larger than that lying outward the foundation. For example, the pore water pressure of points H1, H2 and H3 that lay below the foundation was obviously larger than that of points H4, H5 and H6. It indicated that the existence of the foundation and the superstructure had influence on the increasing of the pore water pressure. The pore pressure ratio of point H1, H2, H3 and H6 reached 1.0 and the sand soil liquefied under the excitation of SJ4. (5) It could be found that the pore pressure ratio time history under excitation of Shanghai Bedrock wave was obviously different from that under El Centro wave. It indicated that the change of the pore water pressure had close relation with the spectral characteristics of the excitation. (6) The pore water pressure did not dissipate immediately after the vibration stop. However, it may continue to increase in a short time (The inputted seismic wave lasted about 8.8s. The time to acquire the data by pore water pressure gauge was about 294.3s). The soil stayed in instable non-linear deformation and the soil surface sank under the excitation. As the vibration stop, the instability could not stop immediately and the deformation continued. That was the reason that the pore water pressure continued to increase after the earthquake.

3.5 The Analysis of Normal Strain Along the Pile and Contact Pressure on the Pile-soil Interface

Strain gauge and soil pressure gauge were arranged along the pile to measure the strain change along the pile and the contact pressure on the pile-soil interface. The arrangement of the measuring points is shown in the Fig.1.

3.5.1. Distribution of the normal strain amplitude along piles

Fig.12 shows the distribution of the normal strain amplitude along the pile under the El Centro wave and

Shanghai Bedrock wave under excitation of different peak acceleration. Some rules could be drawn from the figure as follows.

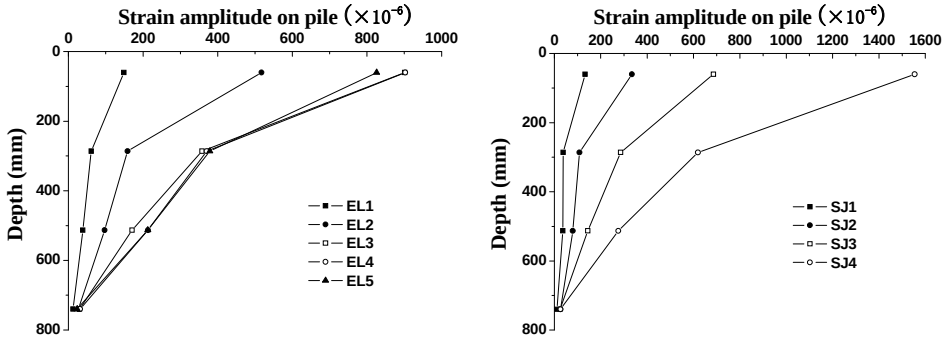

(a) Under excitation of El Centro wave (b) Under excitation of Shanghai Bedrock wave

Fig.12 The distribution of the strain amplitude along piles under excitation of various peak acceleration

(1) The distribution of the strain amplitude along the pile shown that the strain was large at the top of the pile and small at its tip. This was in agreement with the crack distribution observed in the test. The strain amplitude for the pile increased with increasing of input acceleration. (2) The strain amplitude under Shanghai Bedrock wave was smaller than that under El Centro wave when peak acceleration of excitation was smaller. However, the strain amplitude under Shanghai Bedrock wave was bigger than that under El Centro wave when peak acceleration of excitation was bigger. It indicated that the strain amplitude had close relation with the dynamic behavior of the ground and the spectral characteristics of inputted seismic wave.

3.5.2. Distribution of the contact pressure amplitude on the pile-soil interface

Fig.13 shows the distribution of the amplitude of the contact pressure between the soil and piles under the excitation of El Centro wave and Shanghai Bedrock wave with different peak acceleration. Some rules could be drawn from the figure as follows.

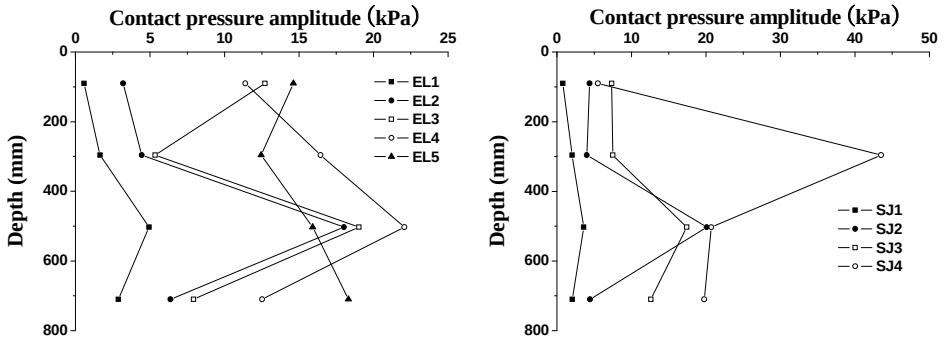

(a) Under excitation of El Centro wave (b) Under excitation of Shanghai Bedrock wave

Fig.13 The distribution of the contact pressure amplitude under excitation of various peak acceleration

(1) The amplitude of the contact pressure was small at the top and bottom of the pile and large at its middle. When the peak acceleration of excitation was smaller, the amplitude of the contact pressure on the soil-pile interface increased basically with increasing of input peak acceleration. However, the contact pressure amplitude decreased as the seismic wave with larger acceleration peak value was inputted. This was the result of the serious rigidity degeneration because of the development of soil liquefaction degree. (2) The value and rule of the contact pressure amplitude under the excitation of El Centro wave was consistent with that under the excitation of Shanghai Bedrock wave. As the seismic wave with smaller peak acceleration was inputted, the strain under Shanghai Bedrock wave was smaller than that under El Centro wave. However, the strain under Shanghai Bedrock wave was larger than that under El Centro wave when the seismic wave with bigger peak acceleration was inputted. It indicated that the strain amplitude had close relation with the dynamic behavior of the ground and the spectral characteristics of seismic wave inputted.

4. CONCLUSION

In this section, the results of the shaking table test on soil-pile-tall building interaction system in ground of soil

liquefaction were analyzed on some aspects, such as experimental phenomena, dynamic characteristics of model, acceleration response, change of pore water pressure, the normal strain along the pile and contact pressure on the pile-soil interface. And some regularity results were concluded.

(1) The phenomenon of practical seismic damage due to soil-pile-tall building interaction in ground of soil liquefaction was reproduced well. (2) The damping ratio of the system was larger than that of the structural material. The mode shape of the SSI system under the liquefied soil was greatly different from that of the structure on the fixed base. (3) Sand magnified vibration under small earthquakes. However, sand soil liquefied, non-linear behavior developed and stiffness declined because of the increasing of the pore water pressure under medium earthquake and strong earthquake. At the time it damped vibration. For the superstructure，the floor peak acceleration was obviously different from each other under small earthquakes. (4) The pore water pressure in the sand soil layer increased quickly with the increasing of the acceleration value under the excitation of either small earthquake or larger earthquake. The pore pressure ratio mainly dissipated after the excitation and the velocity of the dissipation tended to slow gradually from top to bottom. It could also be seen that the transient negative pore pressure occurred when the initial acceleration reached the peak value. For the measuring points at the same depth, the value of the pore water pressure and the pore pressure ratio lying below the foundation was obviously larger than that lying outward the foundation. The pore water pressure did not dissipate immediately after the vibration stop. However, it may continue to increase in a short time. (5) The distribution of the strain amplitude along the pile showed that the strain was large at the top of the pile and small at its tip. The strain amplitude for the pile increased with increasing input acceleration. The distribution of the contact pressure had relation with the peak acceleration of excitation. The amplitude of the contact pressure was small at the top and bottom of the pile and large at its middle. When the peak acceleration of excitation was smaller, the amplitude of the contact pressure on the soil-pile interface increased basically with increasing of input peak acceleration. However, the contact pressure amplitude decreased as the seismic wave with larger acceleration peak value was inputted.

ACKNOWLEDGEMENTS

This project has been carried out under the sponsorship of the project (No. 50578124) of the National Natural Science Foundation of China, the project (No. 07QA14054) of Shanghai Rising-Star Program and the project (No. 2007CB714202) of National Basic Research Program of China.

REFERENCES

Chen, Y.Q., Lu, X.L., Hou, J.G., et al. (2003). Shaking table testing on seismic liquefaction of soft soil under building footing. *Engineering Journal of Wuhan University* **36:1**, 59-64(in Chinese).

Feng, S.L., Wang, J.H., Guo, J.T., et al. (2005). A shake table test on the seismic resistance of pile foundation in liquefied soil. *China Civil Engineering Journal* **38:7**, 92-95(in Chinese).

Funahara, H., Fujii, S. and Tamura, S. (2000). Numerical simulation of pile failure in liquefied soil observed in large-scale shaking table test. *12th World Conference on Earthquake Engineering*, Auckland, New Zealand, No.0927.

Kagawa, T., Minowa, C., Abe, A. (2000). EDUS project (earthquake damage to underground structures). *12th World Conference on Earthquake Engineering*, Auckland, New Zealand, 2000, No.0329.

Ling, X.Z., Guo, M.Z., Wang, D.S., et al. (2006). Large-scale shaking table model test of seismic response of bridge of pile foundation in ground of liquefaction. *Rock and Soil Mechanics* **27:1**, 7-10, 22 (in Chinese).

Lu, X.L., Li, P.Z., Chen, B. et al. (2005). Computer simulation of the dynamic layered soil-pile-structure interaction system. *Canadian Geotechnical Journal* **42:3**, 742-751.

Lu, X.L., Zhang, H.Y., Hu, Z.L., et al. (1999). Shaking table testing of a U-shaped plan building model. *Canada Journal of Civil Engineering* **26:6**, 746-759.

Meng, S.J., Liu, H.L., Yuan, X.M., et al. (2005). Experimental study on the mechanism of earthquake-induced differential settlement of building on liquescent subsoil by shaking table. *Chinese Journal of Rock Mechanics and Engineering* **24:11**, 1978-1985(in Chinese).

Sabnis, G.M., Harris, H.G., White, R.N., et al. (1983). Structural modeling and experimental techniques. Prentice-Hall, Inc., Englewood Cliffs, N.J.

Takahiro, K., Yoichi, Y., Naoki, T., et al. (2004). Shaking table testing of liquefiable ground improved by multi-layer solid. *13th World Conference on Earthquake Engineering*, Vancouver, Canada, Paper No. 136.

Tamura, S., Suzuki, Y., Tsuchiya, T., et al. (2000). Dynamic response and failure mechanisms of a pile foundation during soil liquefaction by shaking table test with a large-scale laminar shear box. *12th World Conference on Earthquake Engineering*, Auckland, New Zealand, 2000, No.0903.